11.5 A 5GHz Resistive-Feedback CMOS LNA for Low-Cost Multi-Standard Applications

Jing-Hong Conan Zhan, Stewart S. Taylor

Intel, Hillsboro, Oregon

Modern CMOS technology has excellent RF performance for applications below 10GHz. Some of this excess performance can be traded for smaller die size and process simplicity, making high-performance RF circuits compatible with digital CMOS technology. Such circuits are important for low-cost, highly integrated communication products, and for multi-standard systems with many radios. In this paper, we describe a 5GHz resistive-feedback LNA with a 2dB NF and 25dB of gain, occupying .025mm^2 of die area in 90nm CMOS technology.

Others have reported resistive-feedback broadband LNAs [1-3], but we improve the NF and return loss through a combination of technology and circuit design. Figure 11.5.1 is a simplified schematic diagram of the LNA. It consists of a g_m-enhanced cascode amplifier M_1-M_2 with source follower feedback buffer M_3. This arrangement results in M_1 and M_2 both having a voltage gain of ~13dB. C_{PFB} compensates for parasitic capacitance C_L and increases the bandwidth. Feedback resistor R_F is DC blocked by C_2. DC bias is provided by a feedback level-shifting source follower circuit (not shown) and isolating resistors R_1 and R_2. This biasing circuit has little impact on AC performance. M_4 is a separate source follower, which would typically form the transconductor in a mixer with R_M when I_{OUT} is taken from its drain. In our case, M_4 interfaces to a 50Ω driver for testing and provides additional reverse isolation.

Input matching at moderate frequencies is set according to

$$R_{in} \cong \frac{R_F}{1+A_V} \cong \frac{R_F}{A_V}. \quad (1)$$

For $R_F \cong 1K\Omega$ and $A_V \cong 20$, $R_{in} \cong 50\Omega$. Matching can be enhanced with off-chip input inductance, such as a bond wire, and/or properly sizing R_L, M_3 and I_3 as explained below. It is well known that the input impedance of the source of M_3 is inductive, given by

$$L_{EQ} \cong C_{gs3}\frac{R_L}{g_{m3}} = \frac{R_L}{2\pi f_{t3}}, \quad (2)$$

where the subscript 3 denotes parameters for M_3. C_2 has a 3% parasitic capacitance to substrate on each side and L_{EQ} can be chosen to resonate with this parasitic capacitance. This additional degree of freedom to fine-tune input matching is used in our design to enhance S_{11} at 1.9GHz. Alternative choices of L_{EQ} can enhance S_{11} at higher frequency, but to a lesser extent.

It can be shown that the noise factor is approximately

$$F \cong 1+\frac{r_t}{R_o}+\frac{R_o}{R_F}+K_1\frac{f_{-3dB}}{f_t} \cong 1+\frac{r_t}{R_o}+\frac{R_o}{R_F}+2\frac{f_{-3dB}}{f_t}. \quad (3)$$

Here, r_t is the sum of all resistors around the input loop including interconnect metal and vias, gate, and source resistance. R_o is the generator resistance. Some portion of the non-quasi-static charging resistance also has noise (h-parameter noise representation), but this is typically small compared to other components in 90nm technology, particularly since it is filtered by gate-source overlap capacitance. K_1, typically ~2, is a factor that captures enhanced channel noise, and noise from R_B, R_L, and M_2. C_F is used to control peaking and also plays some role in S_{11}.

From (2), it is seen that a high f_t and large R_F are desirable for low noise figure. Therefore, a scaled technology with a high f_t contributes to a low noise figure to the extent that r_t is not too large. A large R_F requires high gain, and this trades-off with linearity as the gain of M_1 causes M_2 to be driven by a relatively large signal. The mid-band loop gain of the circuit is

$$T \cong A_v\frac{R_o}{R_f} \cong 1. \quad (4)$$

Equation (4) is set by (1) to achieve a good input match. This small amount of feedback linearizes the LNA. At high frequencies, the loop gain decreases, resulting in degraded IIP_3.

The LNA was fabricated in two 90nm processes. One process is RF enhanced with a high resistivity epi/substrate, metal-insulator-metal (MIM) capacitors and precision poly resistors. The other is a digital process with low epi/substrate resistivity. Although MIM capacitors are available, inter-digitated metal capacitors are used. The circuit was tested with ground-signal-ground probes and an on-chip 50Ω driver. The driver is a modified super source-follower with a series pad output resistor as shown in Figure 11.5.2. The driver bandwidth is 10GHz and, at midband, S_{21} is -7dB and S_{22} is less than -20dB. The driver performance was measured and de-embedded for the measurements presented in Figure 11.5.3. We observe that at 5GHz, S_{11} is -13dB, voltage gain is 25dB, NF is 2dB, and IIP_3 is -14dBm for the RF enhanced process. The performance for the digital process is somewhat worse, except for IIP_3. Much of the reduction in performance for the digital process is due to modeling and extraction errors for the poly resistors in this process. The resistors that were fabricated are ~15% lower than the designed value. The low-resistivity substrate may also play some role.

Figures 11.5.4 and 11.5.5 show the impact of R_F, C_F and C_{PFB} on circuit performance. It was found that these parameters have negligible effect on linearity, and varying R_F by ±12.5% will change the noise figure by ∓0.1dB. Figure 11.5.6 is a table comparing our reported performance to other published data. The power is somewhat high but could be lowered, particularly if less gain and/or bandwidth are required. Note the power in $M4$ would typically be associated with the mixer in a receiver, and is 6.8mW in our design. Figure 11.5.7 is a micrograph of one of the LNAs and output driver.

Acknowledgement:
The authors thank R. Bishop for test set-up and assistance, and K. Soumyanath for support and encouragement.

References:
[1] M. Tiebout, et al., "Low Noise Amplifiers in CMOS, from Device to Circuit Design," *IMS Workshop Slides WSN*, June, 2003.
[2] E. Duvivier, et al., "A Fully Integrated Zero-IF Transceiver for GSM-GPRS Quad-Band Application," *IEEE J. Solid-State Circuits,* vol. 38, pp. 2249-2257, Dec., 2003.
[3] H. Adiseno, et al., "A 1.8-V Wide-Band CMOS LNA for Multiband Multistandard Front-End Receiver," *ESSCIR Dig. Tech Papers,* pp. 141-144, Sept., 2003.

 1-4244-0079-1/06 ©2006 IEEE

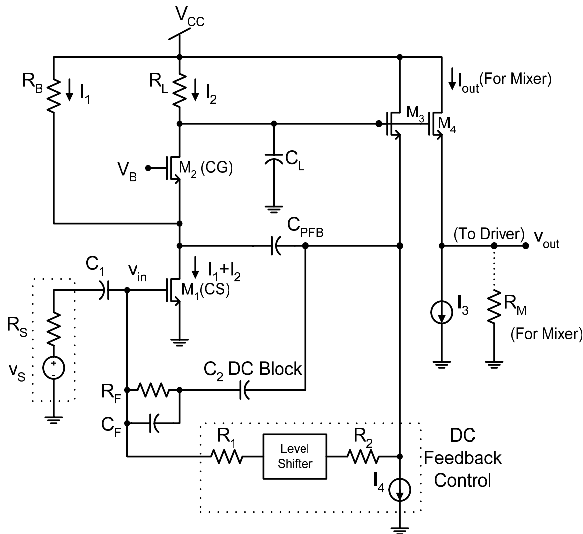

Figure 11.5.1: Simplified LNA schematic diagram.

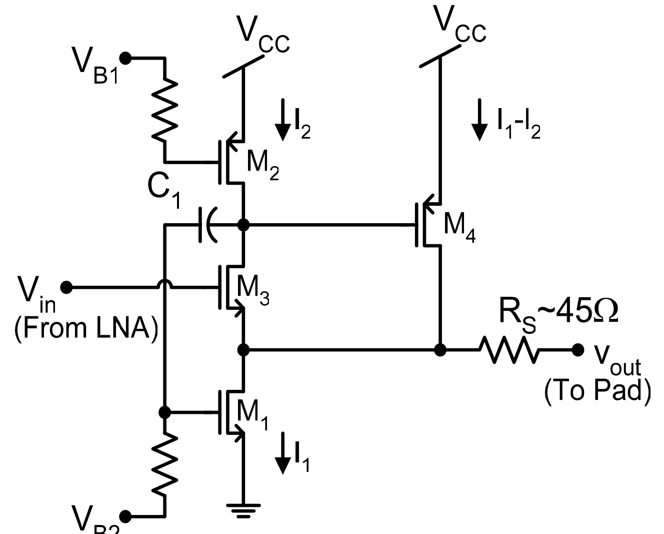

Figure 11.5.2: Simplified driver schematic diagram.

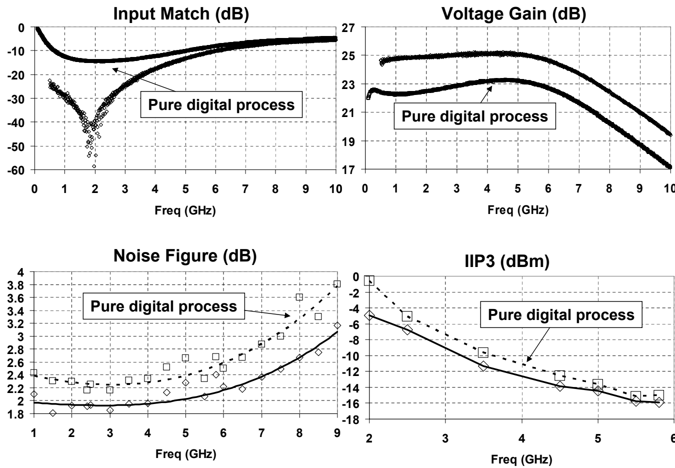

Figure 11.5.3: Measurement.

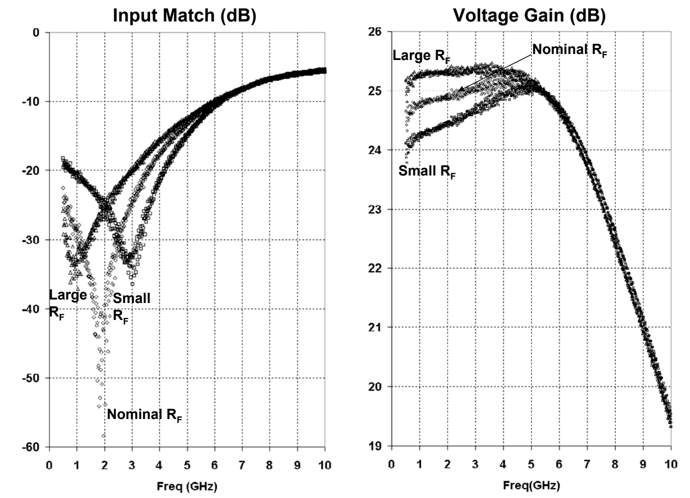

Figure 11.5.4: Effect of R_F.

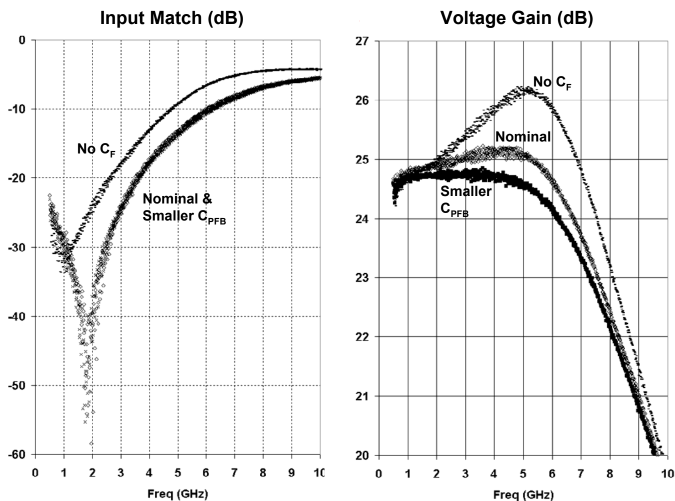

Figure 11.5.5: Effect of C_{PFB} and C_F.

Source	Process	Freq (GHz)	Gain (dB)	NF (dB)	OIP3 (dBm)	Supply (V)	Power (mW)	Active Area (μmxμm)
This Work	90nm CMOS	0.5-8.2	25	1.9-2.6	21@ 2GHz 8.8@5.8GHz	2.7	42	~0.025
JSSC 2005 pp. 1434	90nm CMOS	5.5	13.3	2.9	10.3	1.2	9.72	~0.455
JSSC 2005 pp. 726	180nm CMOS	5.2	16.5	1.11	12.5	1.8	12.4	~0.22
JSSC 2005 pp. 544	180nm CMOS	2-4.6	9.8	2.3	2.8	1.8	12.6	0.9
ISSCC 2005 pp. 534	180nm CMOS	5.8	9.4	2.5	2.2	1.8	3.4	~0.28
JSSC 2004 pp. 275	250nm CMOS	0.2-1.6	13.7	2-2.4	13.7	2.5	35	~0.075
JSSC 2004 pp. 2269	180nm SiGe	3-10	21	2.5-4.2	15.5 @3.5GHz 20 @5.5GHz	3	30	~0.7
JSSC 2004 pp. 2259	180nm CMOS	2.3-9.2	9.3	4	-6.7	1.8	9	~0.66

Figure 11.5.6: Performance summary and comparison.

1-4244-0079-1/06 ©2006 IEEE

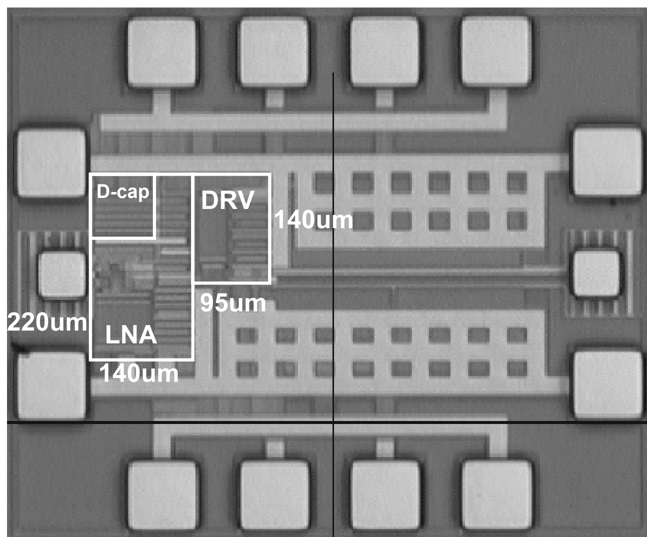

Figure 11.5.7: Chip microraph.

1-4244-0079-1/06 ©2006 IEEE

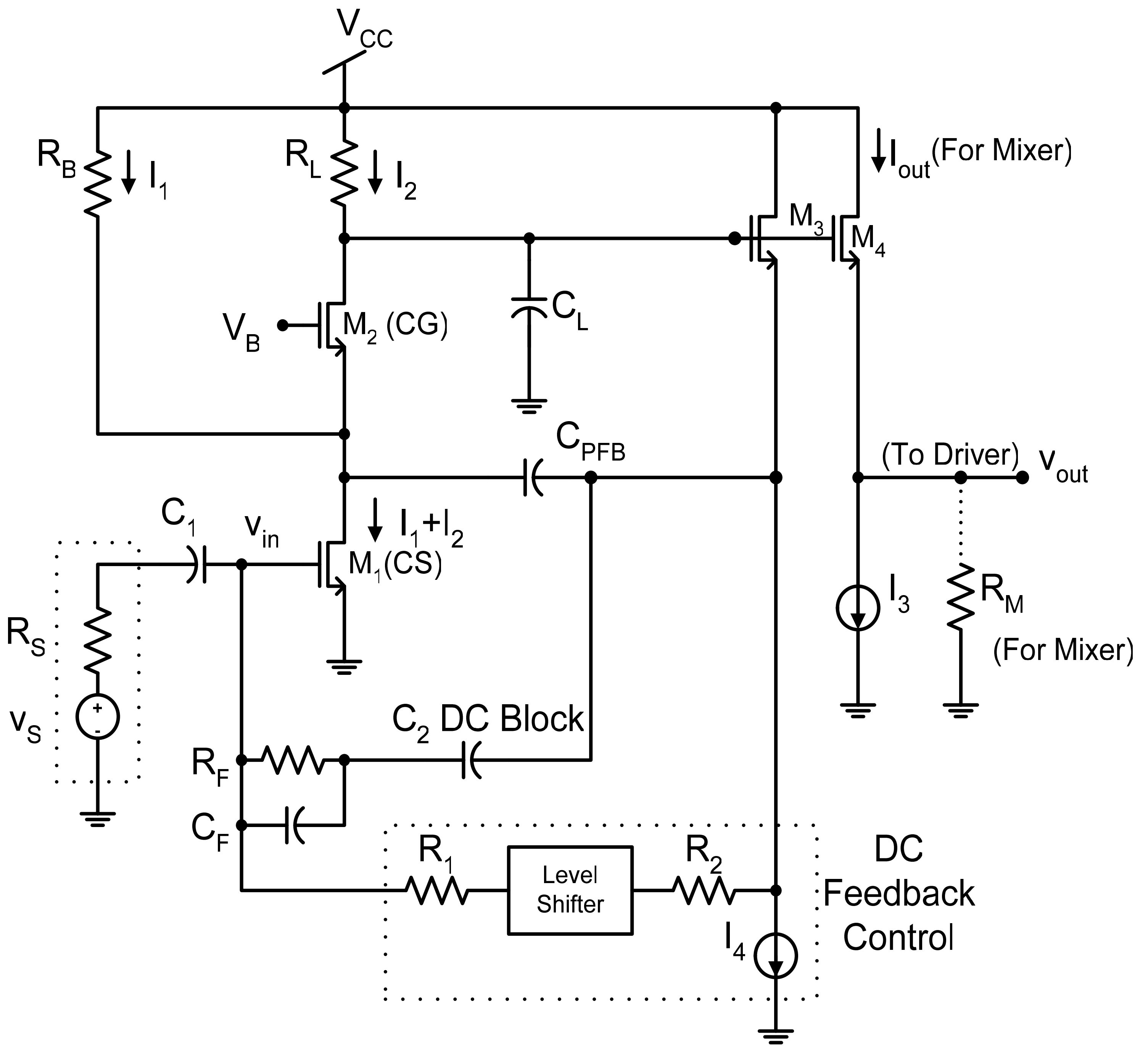

Figure 11.5.1: Simplified LNA schematic diagram.

1-4244-0079-1/06 ©2006 IEEE

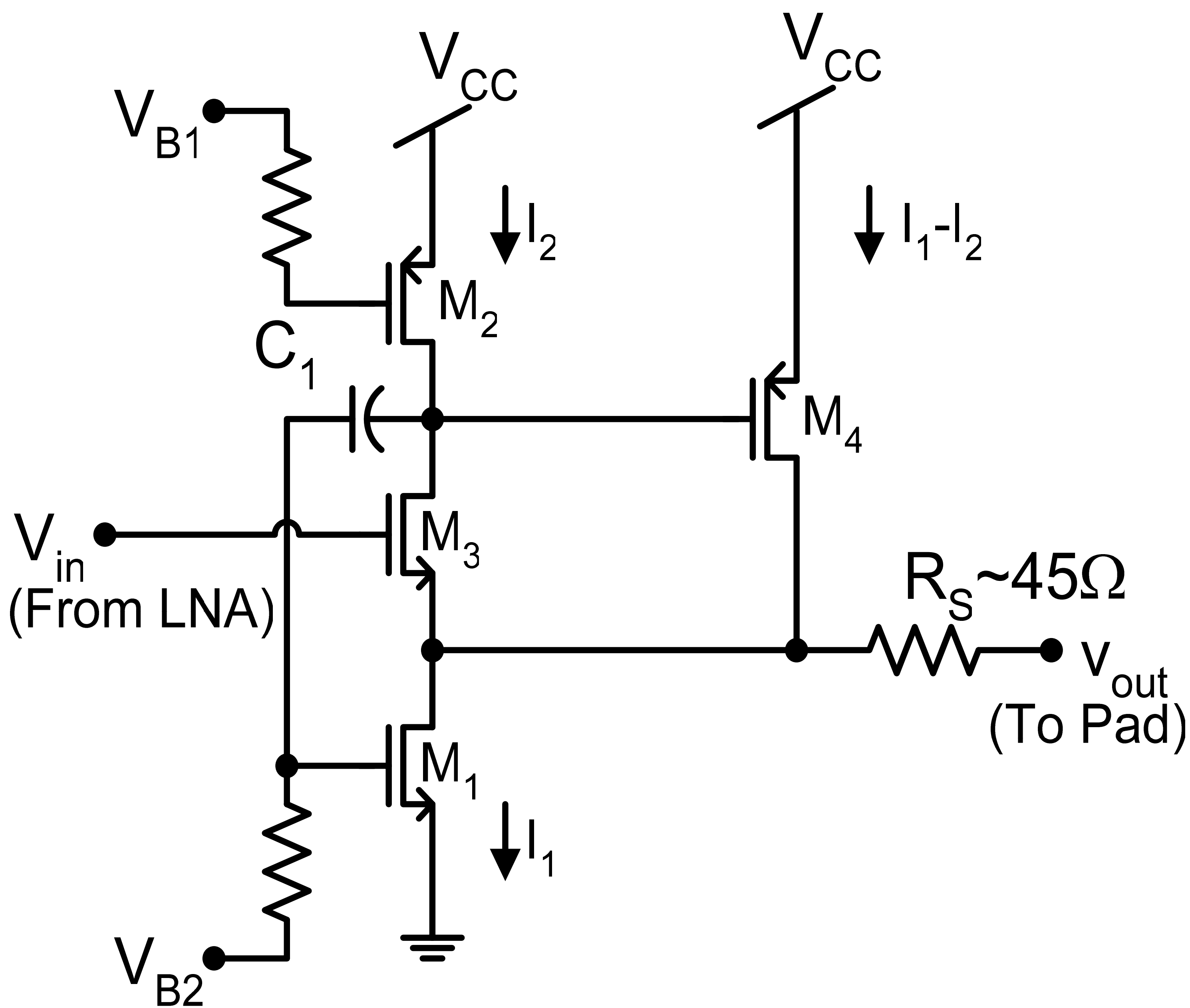

Figure 11.5.2: Simplified driver schematic diagram.

1-4244-0079-1/06 ©2006 IEEE

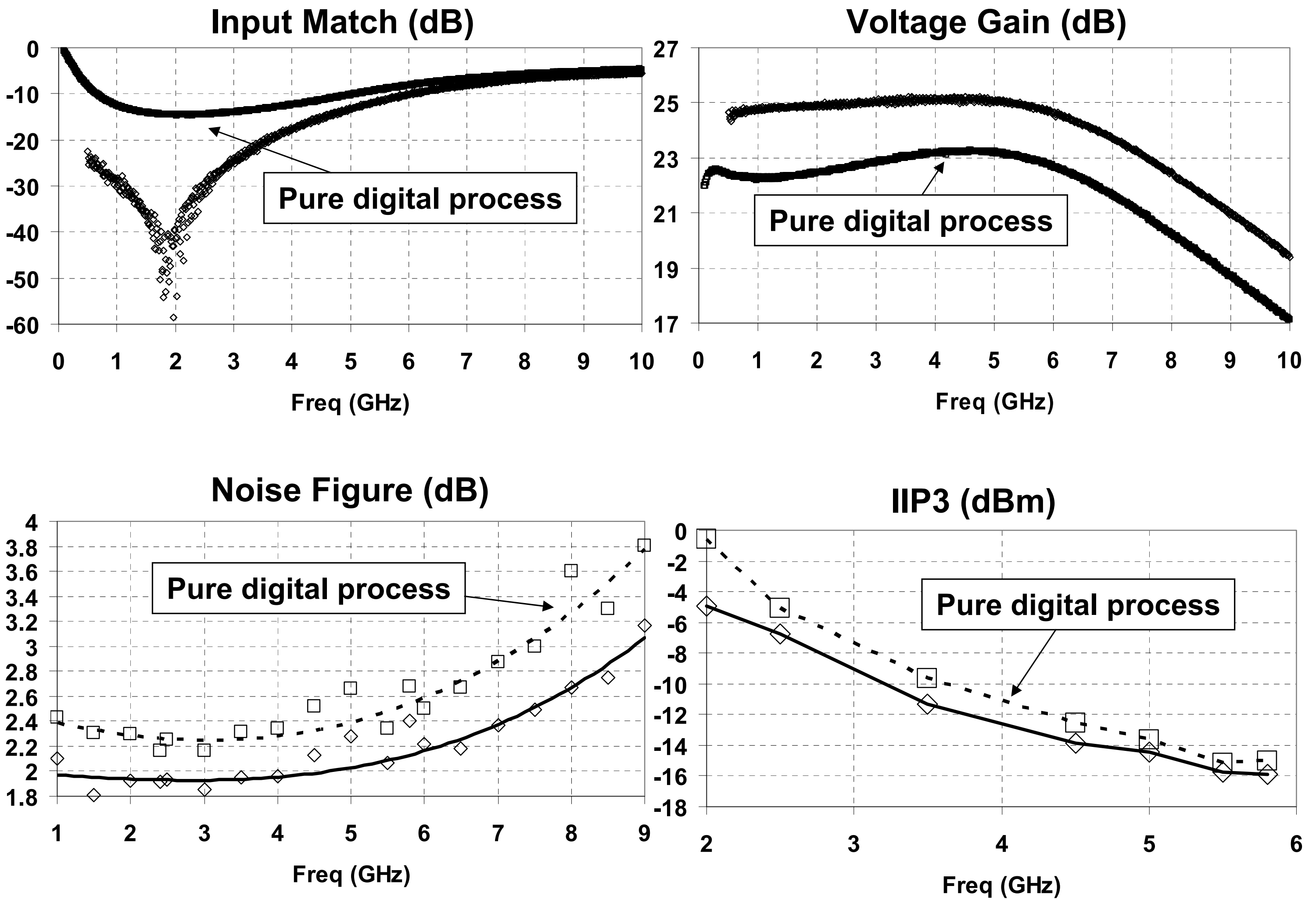

Figure 11.5.3: Measurement.

1-4244-0079-1/06 ©2006 IEEE

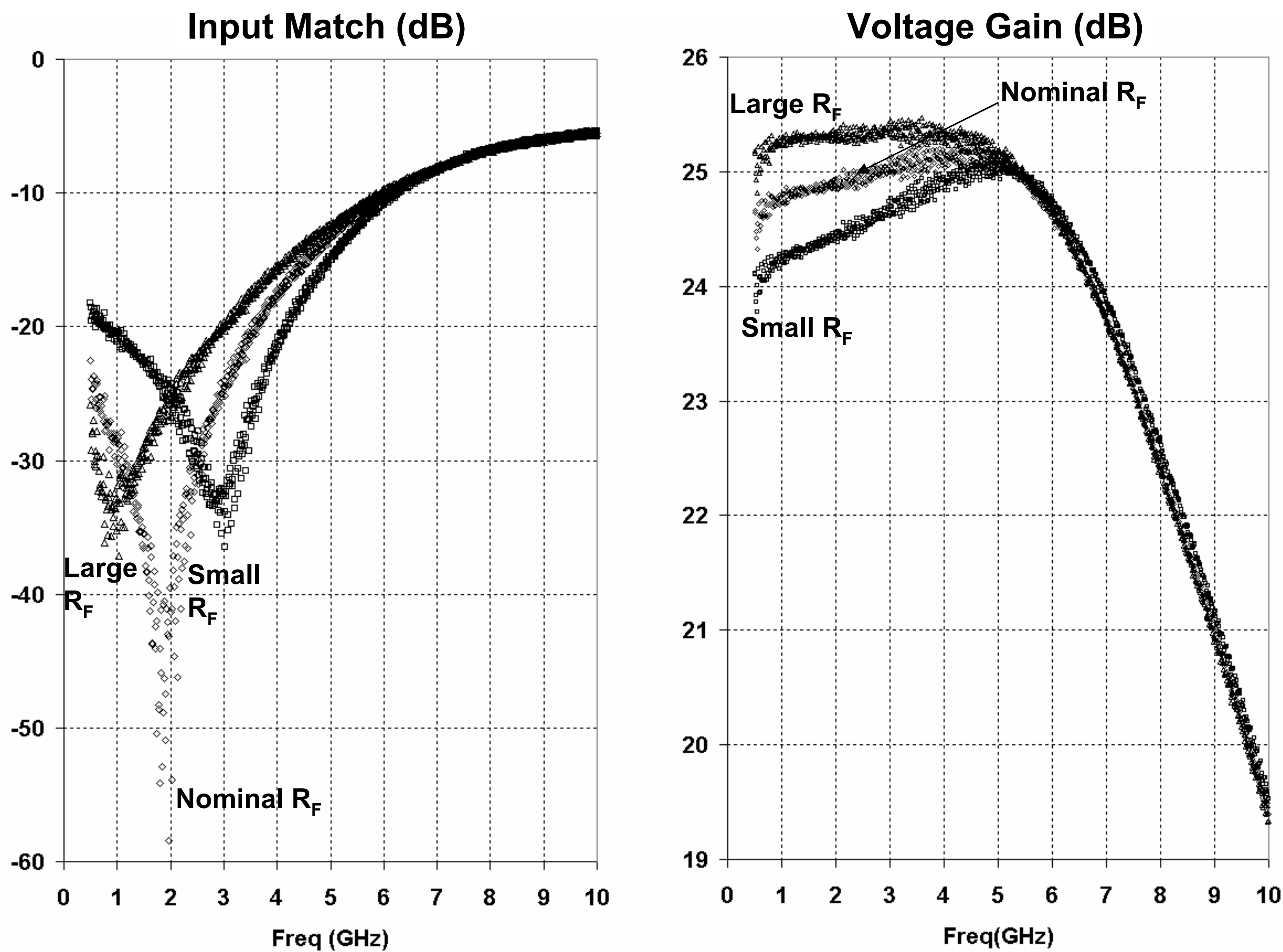

Figure 11.5.4: Effect of R_F.

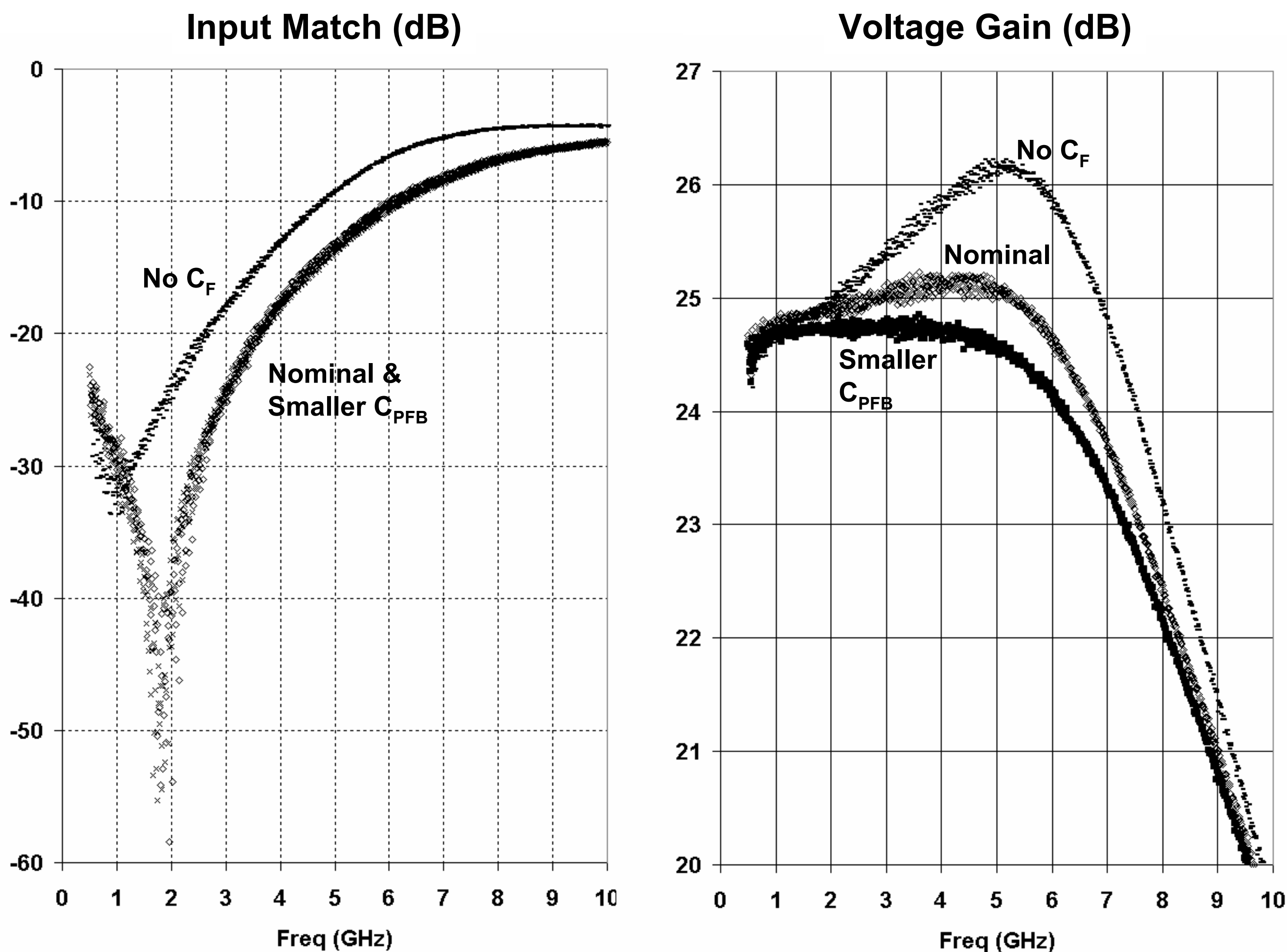

Figure 11.5.5: Effect of C_{PFB} and C_F.

1-4244-0079-1/06 ©2006 IEEE

Source	Process	Freq (GHz)	Gain (dB)	NF (dB)	OIP3 (dBm)	Supply (V)	Power (mW)	Active Area (μmxμm)
This Work	90nm CMOS	0.5-8.2	25	1.9-2.6	21@ 2GHz 8.8@5.8GHz	2.7	42	~0.025
JSSC 2005 pp. 1434	90nm CMOS	5.5	13.3	2.9	10.3	1.2	9.72	~0.455
JSSC 2005 pp. 726	180nm CMOS	5.2	16.5	1.11	12.5	1.8	12.4	~0.22
JSSC 2005 pp. 544	180nm CMOS	2-4.6	9.8	2.3	2.8	1.8	12.6	0.9
ISSCC 2005 pp. 534	180nm CMOS	5.8	9.4	2.5	2.2	1.8	3.4	~0.28
JSSC 2004 pp. 275	250nm CMOS	0.2-1.6	13.7	2-2.4	13.7	2.5	35	~0.075
JSSC 2004 pp. 2269	180nm SiGe	3-10	21	2.5-4.2	15.5 @3.5GHz 20 @5.5GHz	3	30	~0.7
JSSC 2004 pp. 2259	180nm CMOS	2.3-9.2	9.3	4	-6.7	1.8	9	~0.66

Figure 11.5.6: Performance summary and comparison.

1-4244-0079-1/06 ©2006 IEEE

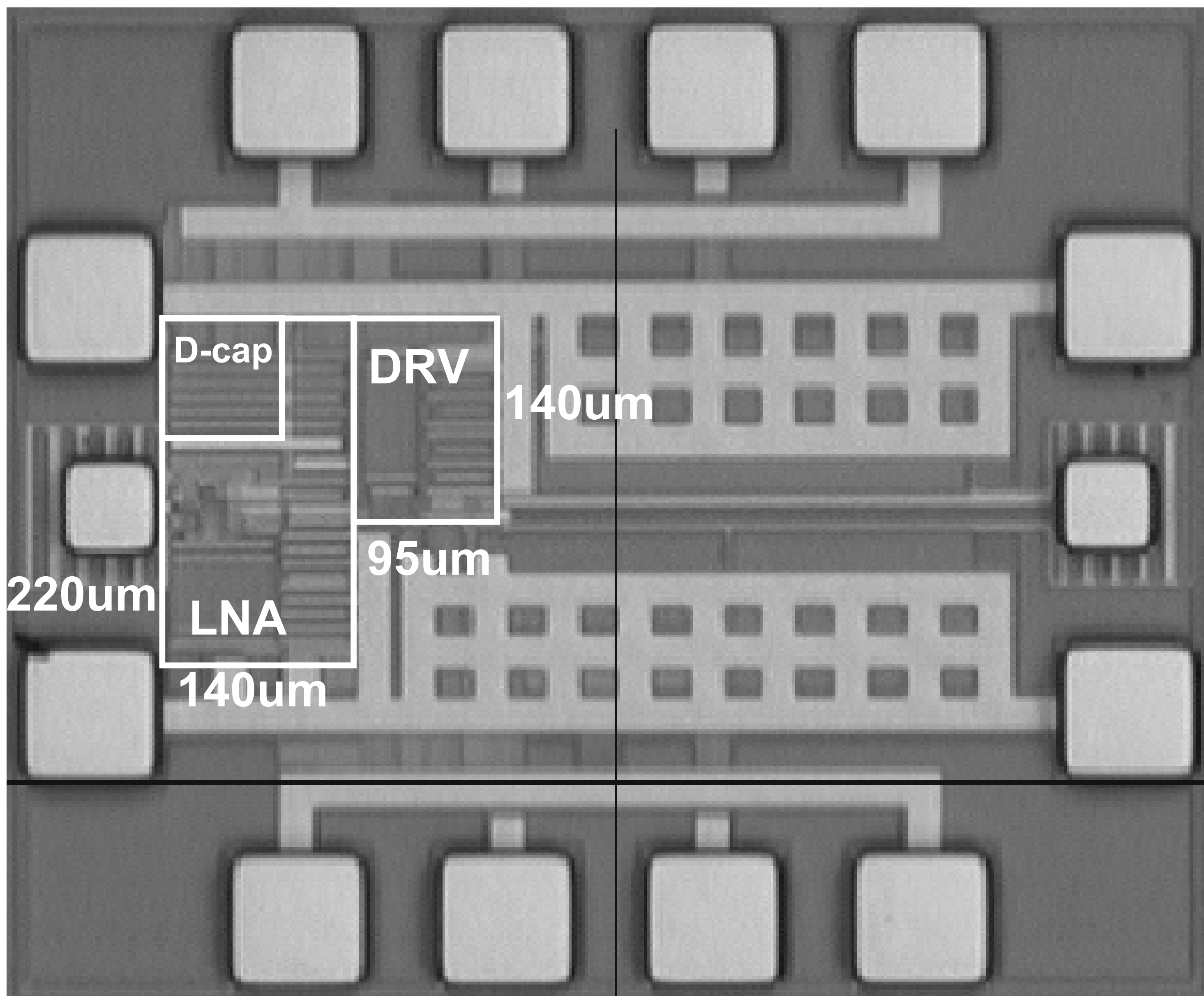

Figure 11.5.7: Chip microraph.

1-4244-0079-1/06 ©2006 IEEE